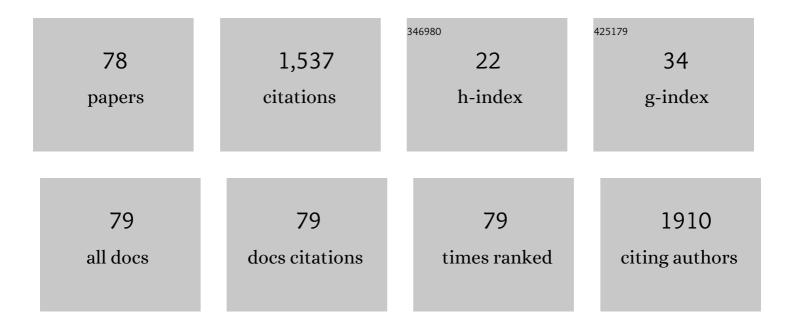
List of Publications by Year in descending order

Source: https://exaly.com/author-pdf/9485416/publications.pdf Version: 2024-02-01



MINC-YUL

#	Article	IF	CITATIONS
1	Significantly improved photo carrier injection by the MoS2/ZnO/HNP hybrid UV photodetector architecture. Applied Surface Science, 2022, 574, 151739.	3.1	22
2	High performance hybrid MXene nanosheet/CsPbBr3 quantum dot photodetectors with an excellent stability. Journal of Alloys and Compounds, 2022, 895, 162570.	2.8	21
3	High performance ZnO quantum dot (QD)/ magnetron sputtered ZnO homojunction ultraviolet photodetectors. Applied Surface Science, 2022, 582, 152352.	3.1	16
4	MoS ₂ Nanoflake and ZnO Quantum Dot Blended Active Layers on AuPd Nanoparticles for UV Photodetectors. ACS Applied Nano Materials, 2022, 5, 3289-3302.	2.4	9
5	Efficient Infrared Solar Cells Employing Quantum Dot Solids with Strong Interâ€Dot Coupling and Efficient Passivation. Advanced Functional Materials, 2021, 31, 2006864.	7.8	16
6	Facile Fabrication of Ultrasensitive Honeycomb Nano-Mesh Ultraviolet Photodetectors Based on Self-Assembled Plasmonic Architectures. ACS Applied Materials & Interfaces, 2021, 13, 35972-35980.	4.0	9
7	Efficiently Passivated PbSe Quantum Dot Solids for Infrared Photovoltaics. ACS Nano, 2021, 15, 3376-3386.	7.3	32
8	Hybrid Device Architecture Using Plasmonic Nanoparticles, Graphene Quantum Dots, and Titanium Dioxide for UV Photodetectors. ACS Applied Materials & Interfaces, 2021, 13, 3408-3418.	4.0	36
9	ZnO Quantum Dot/MXene Nanoflake Hybrids for Ultraviolet Photodetectors. ACS Applied Nano Materials, 2021, 4, 13674-13682.	2.4	21
10	Controllable 3D plasmonic nanostructures for high-quantum-efficiency UV photodetectors based on 2D and 0D materials. Materials Horizons, 2020, 7, 905-911.	6.4	16
11	Enhanced Spatial Light Confinement of All Inorganic Perovskite Photodetectors Based on Hybrid Plasmonic Nanostructures. Small, 2020, 16, e2004234.	5.2	17
12	Self-Assembled Al Nanostructure/ZnO Quantum Dot Heterostructures for High Responsivity and Fast UV Photodetector. Nano-Micro Letters, 2020, 12, 114.	14.4	43
13	Highly thermally stable Au–Al bimetallic conductive thin films with a broadband transmittance between UV and NIR regions. Journal of Materials Chemistry C, 2020, 8, 2852-2860.	2.7	6
14	Electro-thermal synergetic effect in 0.94Bi0.5Na0.5TiO3-0.06BaZr0.2Ti0.8O3: ZnO pyroelectric composites for high-performance thermal energy harvesting. Applied Physics Letters, 2019, 115, .	1.5	5
15	Thermal energy harvesting performance in 0.94Bi0.5Na0.5TiO3-0.06BaZr0.2Ti0.8O3: AlN composite ceramics based on the Olsen cycle. Journal of the European Ceramic Society, 2019, 39, 5243-5251.	2.8	17
16	Ultrahigh Responsivity UV Photodetector Based on Cu Nanostructure/ZnO QD Hybrid Architectures. Small, 2019, 15, e1901606.	5.2	42
17	Significantly enhanced ferroelectric and pyroelectric properties in polyvinylidene fluoride induced by shear force with spin-coating. Journal of Materials Science: Materials in Electronics, 2019, 30, 12540-12544.	1.1	6
18	Hexagonal boron nitride nanosheets doped pyroelectric ceramic composite for high-performance thermal energy harvesting. Nano Energy, 2019, 60, 144-152.	8.2	34

#	Article	IF	CITATIONS
19	Controllable MXene nano-sheet/Au nanostructure architectures for the ultra-sensitive molecule Raman detection. Nanoscale, 2019, 11, 22230-22236.	2.8	32
20	Nanoconfinementâ€Induced Giant Electrocaloric Effect in Ferroelectric Polymer Nanowire Array Integrated with Aluminum Oxide Membrane to Exhibit Record Cooling Power Density. Advanced Materials, 2019, 31, e1806642.	11.1	56
21	High room-temperature pyroelectric property in lead-free BNT-BZT ferroelectric ceramics for thermal energy harvesting. Journal of the European Ceramic Society, 2019, 39, 1810-1818.	2.8	59
22	Determination of growth regimes of Pt nanostructures on GaN (0001) based on the control of Pt thickness and annealing time: Morphological evolution of Pt nanostructures from the nanoparticles, nanoclusters to porous network. Proceedings of the Institution of Mechanical Engineers, Part L: Journal of Materials: Design and Applications, 2019, 233, 913-923.	0.7	0
23	Improved heat transfer for pyroelectric energy harvesting applications using a thermal conductive network of aluminum nitride in PMN–PMS–PZT ceramics. Journal of Materials Chemistry A, 2018, 6, 5040-5051.	5.2	45
24	Morphological, Structural and Optical Evolution of Ag Nanostructures on c-Plane GaN Through the Variation of Deposition Amount and Temperature. Metals and Materials International, 2018, 24, 337-350.	1.8	4
25	Effects of Fe and Al co-doping on the leakage current density and clamp voltage ratio of ZnO varistor. Journal of Alloys and Compounds, 2018, 747, 1018-1026.	2.8	19
26	Lead-free Ba(1-x)SrxTiO3 ceramics for room-temperature pyroelectric energy conversion. Ceramics International, 2018, 44, 8270-8276.	2.3	21
27	Investigation on the morphology and optical properties of self-assembled Ag Nanostructures on <mml:math <br="" display="inline" id="mml17" xmlns:mml="http://www.w3.org/1998/Math/MathML">overflow="scroll" altimg="si17.gif"><mml:mi>c</mml:mi></mml:math> -plane GaN by the control of annealing temperature and duration. Nano Structures Nano Objects. 2018, 15, 28-39.	1.9	7
28	Harvesting Energy from Human Activity: Ferroelectric Energy Harvesters for Portable, Implantable, and Biomedical Electronics. Energy Technology, 2018, 6, 791-812.	1.8	49
29	Facile fabrication of configuration controllable self-assembled Al nanostructures as UV SERS substrates. Nanoscale, 2018, 10, 22737-22744.	2.8	22
30	Broad-Band High-Sensitivity ZnO Colloidal Quantum Dots/Self-Assembled Au Nanoantennas Heterostructures Photodetectors. ACS Applied Materials & Interfaces, 2018, 10, 32516-32525.	4.0	45
31	High thermal stability in PLZST anti-ferroelectric energy storage ceramics with the coexistence of tetragonal and orthorhombic phase. Journal of the European Ceramic Society, 2018, 38, 5396-5401.	2.8	48
32	Ultra Uniform Pb0.865La0.09(Zr0.65Ti0.35)O3 Thin Films with Tunable Optical Properties Fabricated via Pulsed Laser Deposition. Materials, 2018, 11, 525.	1.3	1
33	Effect of Annealing Temperature on Morphological and Optical Transition of Silver Nanoparticles on c-Plane Sapphire. Journal of Nanoscience and Nanotechnology, 2018, 18, 3466-3477.	0.9	8
34	Mechanical force-driven growth of elongated BaTiO3 lead-free ferroelectric nanowires. Ceramics International, 2017, 43, 2969-2973.	2.3	15
35	Enhanced energy density of polymer nanocomposites at a low electric field through aligned BaTiO ₃ nanowires. Journal of Materials Chemistry A, 2017, 5, 6070-6078.	5.2	175
36	Study on the dimensional, configurational and optical evolution of palladium nanostructures on c -plane sapphire by the control of annealing temperature and duration. Applied Surface Science, 2017, 416, 1-13	3.1	14

#	Article	IF	CITATIONS
37	Fabrication of Ag nanostructures by the systematic control of annealing temperature and duration on GaN (0001) via the solid state dewetting. Physica Status Solidi (A) Applications and Materials Science, 2017, 214, 1600702.	0.8	6
38	High electrocaloric effect in hotâ€pressed Pb _{0.85} La _{0.1} (Zr _{0.65} Ti _{0.35})O ₃ ceramics with a wide operating temperature range. Journal of the American Ceramic Society, 2017, 100, 4581-4589.	1.9	30
39	Effect of Systematic Control of Pd Thickness and Annealing Temperature on the Fabrication and Evolution of Palladium Nanostructures on Si (111) via the Solid State Dewetting. Nanoscale Research Letters, 2017, 12, 364.	3.1	12
40	Determination of growth regimes of Pd nanostructures on c-plane sapphire by the control of deposition amount at different annealing temperatures. Physical Chemistry Chemical Physics, 2017, 19, 15084-15097.	1.3	11
41	Effect of Zr/Ti ratio on microstructure and electrical properties of pyroelectric ceramics for energy harvesting applications. Journal of Alloys and Compounds, 2017, 710, 869-874.	2.8	28
42	Morphological and Optical Evolution of Silver Nanoparticles on Sapphire (0001) Along With the Concurrent Influence of Diffusion, Ostwald's Ripening, and Sublimation. IEEE Nanotechnology Magazine, 2017, 16, 321-332.	1.1	12
43	Tuning the configuration of Au nanostructures: from vermiform-like, rod-like, triangular, hexagonal, to polyhedral nanostructures on c-plane GaN. Journal of Materials Science, 2017, 52, 391-407.	1.7	16
44	Various Silver Nanostructures on Sapphire Using Plasmon Self-Assembly and Dewetting of Thin Films. Nano-Micro Letters, 2017, 9, 17.	14.4	36
45	Boron and sodium co-doped ZnO varistor with high stability of pulse current surge. Journal of Alloys and Compounds, 2017, 728, 368-375.	2.8	10
46	Fabrication and determination of growth regimes of various Pd NPs based on the control of deposition amount and temperature on c-plane GaN. Journal of Materials Research, 2017, 32, 3593-3604.	1.2	1
47	Enhanced sensitivity and response speed of graphene oxide/ZnO nanorods photodetector fabricated by introducing graphene oxide in seed layer. Journal of Materials Science: Materials in Electronics, 2017, 28, 15891-15898.	1.1	10
48	Molybdenum and tungsten doped SnO ₂ transparent conductive thin films with broadband high transmittance between the visible and near-infrared regions. CrystEngComm, 2017, 19, 4413-4423.	1.3	27
49	Geometrical influence of conducting fillers on the dielectric tunable properties of antiferroelectric ceramic/conducting filler/polystyrene composites under low electric field. Journal of Materials Science: Materials in Electronics, 2017, 28, 10184-10190.	1.1	1
50	Au-assisted fabrication of nano-holes on c-plane sapphire via thermal treatment guided by Au nanoparticles as catalysts. Applied Surface Science, 2017, 393, 23-29.	3.1	22
51	Effects of annealing temperature and duration on the morphological and optical evolution of self-assembled Pt nanostructures on c-plane sapphire. PLoS ONE, 2017, 12, e0177048.	1.1	24
52	Nanoscale morphology and optical property evolution of Pt nanostructures on GaN (0 0 0 1) by the systematic control of annealing temperature and duration with various Pt thickness. Materials Research Express, 2017, 4, 065019.	0.8	6
53	Evolution of morphological and optical properties of self-assembled Ag nanostructures on <i>c</i> -plane sapphire (0001) by the precise control of deposition amount. Materials Research Express, 2016, 3, 125006.	0.8	6
54	Precise control of configuration, size and density of self-assembled Au nanostructures on 4H-SiC (0001) by systematic variation of deposition amount, annealing temperature and duration. CrystEngComm, 2016, 18, 3347-3357.	1.3	20

#	Article	IF	CITATIONS
55	Nanoparticles to Nanoholes: Fabrication of Porous GaN with Precisely Controlled Dimension via the Enhanced GaN Decomposition by Au Nanoparticles. Crystal Growth and Design, 2016, 16, 3334-3344.	1.4	18
56	Ag Nanostructures on GaN (0001): Morphology Evolution Controlled by the Solid State Dewetting of Thin Films and Corresponding Optical Properties. Crystal Growth and Design, 2016, 16, 6974-6983.	1.4	9
57	Systematic control of the size, density and configuration of Pt nanostructures on sapphire (0 0 0 1) by the variation of deposition amount and dwelling time. Applied Surface Science, 2016, 368, 198-207.	3.1	39
58	From the Au nano-clusters to the nanoparticles on 4H-SiC (0001). Scientific Reports, 2015, 5, 13954.	1.6	22
59	Systematic Control of Self-Assembled Au Nanoparticles and Nanostructures Through the Variation of Deposition Amount, Annealing Duration, and Temperature on Si (111). Nanoscale Research Letters, 2015, 10, 380.	3.1	16
60	Evolution of Self-Assembled Au NPs by Controlling Annealing Temperature and Dwelling Time on Sapphire (0001). Nanoscale Research Letters, 2015, 10, 494.	3.1	15
61	Systematic Study on the Self-Assembled Hexagonal Au Voids, Nano-Clusters and Nanoparticles on GaN (0001). PLoS ONE, 2015, 10, e0134637.	1.1	23
62	Configuration, Dimension and Density Control of 3-D Gold Nanostructures on Various Type-B GaAs Surfaces by the Systematic Variation of Annealing Temperature, Annealing Duration and Deposition Amount. 3D Research, 2015, 6, 1.	1.8	1
63	Shape transformation of self-assembled Au nanoparticles by the systematic control of deposition amount on sapphire (0001). RSC Advances, 2015, 5, 66212-66220.	1.7	21
64	Observation of Shape, Configuration, and Density of Au Nanoparticles on Various GaAs Surfaces via Deposition Amount, Annealing Temperature, and Dwelling Time. Nanoscale Research Letters, 2015, 10, 950.	3.1	11
65	Control of size and density of self-assembled Au droplets via systematic deposition amount control on high-index GaAs type-A surfaces. Japanese Journal of Applied Physics, 2014, 53, 095502.	0.8	1
66	Nucleation, transition, and maturing of the self-assembled Au droplets on various type-A GaAs substrates. Journal of Applied Physics, 2014, 116, 084301.	1.1	3
67	Effect of annealing temperature on the fabrication of self-assembled gold droplets on various type-B GaAs surfaces. CrystEngComm, 2014, 16, 4390.	1.3	9
68	Droplets to Merged Nanostructures: Evolution of Gold Nanostructures by the Variation of Deposition Amount on Si(111). Crystal Growth and Design, 2014, 14, 1128-1134.	1.4	11
69	Effect of Au thickness on the evolution of self-assembled Au droplets on GaAs (111)A and (100). Nanoscale Research Letters, 2014, 9, 407.	3.1	4
70	Fabrication of self-assembled Au droplets by the systematic variation of the deposition amount on various type-B GaAs surfaces. Nanoscale Research Letters, 2014, 9, 436.	3.1	2
71	From the nucleation of wiggling Au nanostructures to the dome-shaped Au droplets on GaAs (111)A, (110), (100), and (111)B. Nanoscale Research Letters, 2014, 9, 113.	3.1	5
72	Mini droplets to super droplets: evolution of self-assembled Au droplets on GaAs(111)B and (110). Journal of Applied Crystallography, 2014, 47, 505-510.	1.9	13

#	Article	IF	CITATIONS
73	Annealing temperature effect on self-assembled Au droplets on Si (111). Nanoscale Research Letters, 2013, 8, 525.	3.1	31
74	Observation of Ga Metal Droplet Formation on Photolithographically Patterned GaAs (100) Surface by Droplet Epitaxy. IEEE Nanotechnology Magazine, 2012, 11, 985-991.	1.1	11
75	Formation of Ga droplets on patterned GaAs (100) by molecular beam epitaxy. Nanoscale Research Letters, 2012, 7, 550.	3.1	3
76	Sharp contrast of the density and size of Ga metal droplets on photolithographically patterned GaAs (100) by droplet epitaxy under an identical growth environment. Physica Status Solidi (A) Applications and Materials Science, 2012, 209, 1075-1079.	0.8	2
77	Inside Back Cover: Sharp contrast of the density and size of Ga metal droplets on photolithographically patterned GaAs (100) by droplet epitaxy under an identical growth environment (Phys. Status Solidi A 6/2012). Physica Status Solidi (A) Applications and Materials Science, 2012, 209, n/a-n/a.	0.8	0
78	Increased Light Trapping by Surface Nano-Structuring on Si Using Multi-Walled Carbon Nanotubes Mask Etching Technique. Journal of Nanoelectronics and Optoelectronics, 2012, 7, 311-316.	0.1	0